Airborne Signal Intercept for Wide-Area Battlefield Surveillance

Larry L. Horowitz

■ **This article discusses the wide-area monitoring of enemy battlefield communications by a standoff aircraft. The purpose of this activity is to detect enemy emitters, determine their directions, and, when possible, copy their signals. Difficulties arise, however, because in typical battlefield scenarios many simultaneous communication emitters use frequency channels in the low VHF band (30 to 88 MHz). At this frequency band, the conventional antenna aperture available to the monitoring aircraft platform is only a few wavelengths long, leading to a broad receiving beamwidth and heavy cochannel interference. We discuss superresolution techniques that overcome the cochannel interference to improve the direction finding and copying of signals of interest. We also discuss improvements that can be obtained by knowing about the classes of signals being transmitted or by enhancing the antenna-array calibration of the airborne antenna. These techniques can be used to upgrade current signal intercept systems.**

T HE ABILITY TO PERFORM direction finding and signal copy of enemy battlefield-communication emitters received by a standoff aircraft provides a tactical advantage during wartime. Most field communications—friendly and unfriendly—occur in the low VHF band (30 to 88 MHz) for mobile local networking, and utilize primarily vertical polarization. At this frequency band, ground-communication signals can penetrate foliage and diffract around objects so that a communicator behind an obstruction can still communicate over the local network. Such low frequencies also allow for low-cost omnidirectional antennas of practical size that provide good signal-to-noise ratio (SNR) for the field units. Because of the limited spectrum available at this low VHF band, field units reuse narrowband (25 kHz) frequency channels over the battlefield without serious interference because the propagation losses for long-range ground-to-ground communications are typically high. Consequently, several communication nets can use the same frequency at the same time.

These features of low VHF communications, while effective for ground-to-ground communications, complicate the problem of wide-area detection, direction finding, and signal copy from a standoff aircraft. Figure 1 shows a standoff aircraft conducting wide-area battlefield surveillance. The aircraft, which has its physical antenna dimension limited to a few wavelengths of the received frequency, operates at a high altitude to hear the communications of all the nets simultaneously and hence monitors the emitters of interest under conditions of high cochannel interference. Further complicating the problem is that friendly emitters closer to the aircraft than the signal of interest are typically received more strongly than the signal of interest.

Figure 2 shows a simplified geometry of what the standoff aircraft receives on one 25-kHz frequency channel of the low VHF band. At this frequency, the signal wavelength is comparable to the length of the biggest array that can be placed on the aircraft, so the receiver beamwidth is wide. Under these circum-
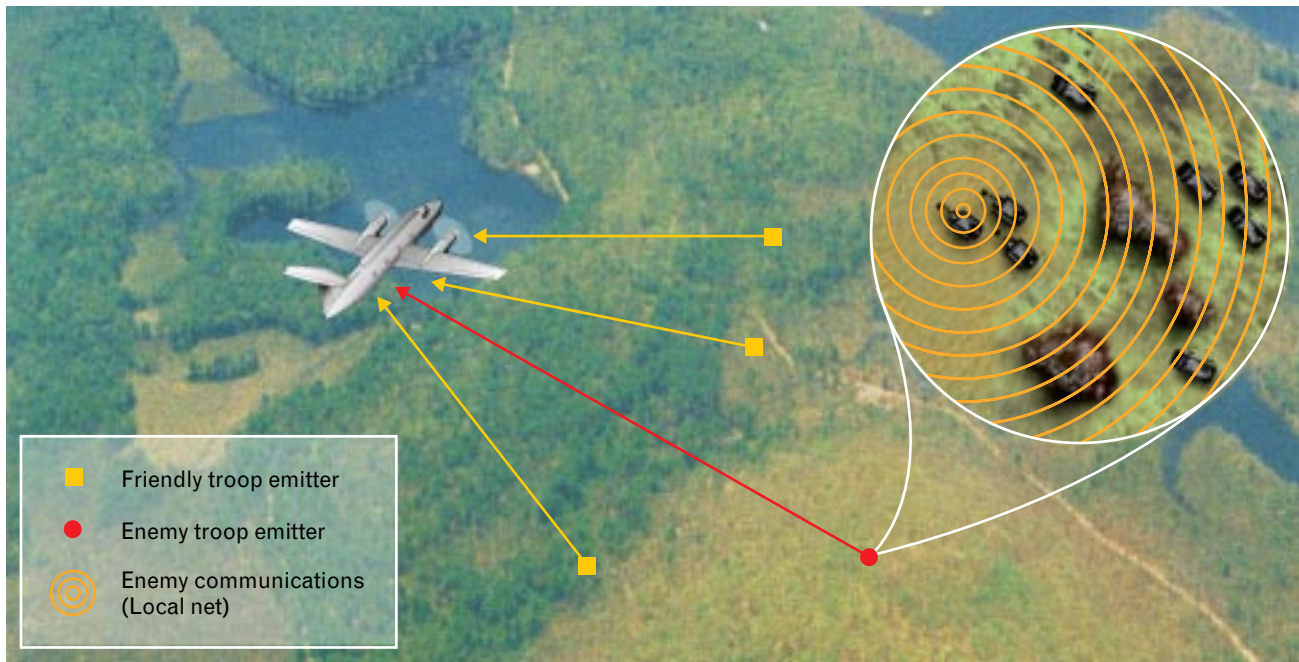
FIGURE 1. Wide-area monitoring of enemy battlefield communications by a standoff aircraft. Most field communications occur in the low VHF band (30 to 88 MHz) for mobile local networking. Several communication nets can use the same narrowband frequency channel at the same time because the long-range ground-to-ground propagation losses are high. The aircraft operates at a high altitude to hear the communications of all the nets simultaneously, and must monitor the emitter of interest under conditions of high cochannel interference.

stances, conventional beamsteering techniques that direct the main beam in search of signals are not desirable because they force us to hear all the emitters at once. As a result, current wide-area intercept systems cannot direction-find and copy the signal of interest unless it is the strongest signal in the channel, an unlikely battlefield situation. To isolate the signal of interest, we must apply superresolution signal processing to narrow the resolution of the receiver beam.

In the next section, we discuss how direction finding and signal copy may be modeled as parameter-estimation problems solved by signal processing algorithms. Then we consider direction finding and signal copy in the most basic scenario, in which no prior knowledge of the waveforms is assumed but some array-calibration knowledge is available. We examine the benefits of prior knowledge of the waveform classes and enhanced array calibration, and highlight some of the technical problems that were solved in the development of the signal processing algorithms.

Direction-finding and signal-copy results are presented from an airborne technology demonstration

system developed at Lincoln Laboratory. Successful direction finding and signal copy is achieved with emitters separated by as little as one-tenth of the natural beamwidth of the antenna array. We conclude that given one to three wavelengths of aperture and four to eight antenna elements, successful detection, direction finding, and signal copy can be achieved for all signal types in the low VHF band.

Direction Finding and Signal Copy as Parameter-Estimation Problems

The tasks of direction-finding and copying a signal can be treated as a parameter-estimation problem. The parameters that we wish to estimate—emitter signals and their directions—are derived from observations that depend on these parameters. To estimate these parameters, we must model how the measurements depend on the parameters. As a starting point for our model, we look at the geometry of an emitter signal received at an aircraft with four antennas, as shown in Figure 3. The emitter transmits a time-dependent signal $a(t)$, which arrives at an off-broadside
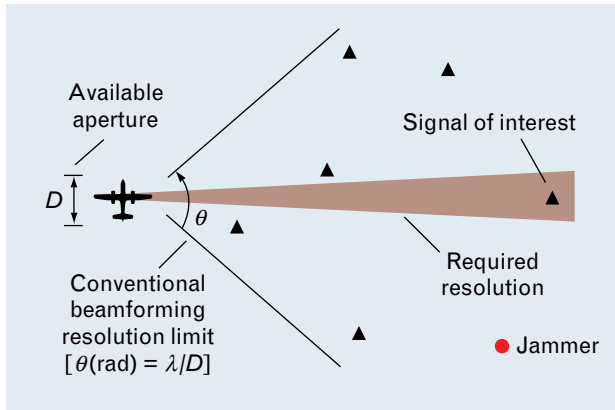
FIGURE 2. Signal reception at the standoff aircraft. A battlefield environment on one 25-kHz channel can include three to eight emitters, most friendly, each communicating with a local network (black triangles). Noncombatant emitters and jammers can also transmit over the same channel. Because conventional beamsteering techniques force us to hear all the emitters at once, we must apply superresolution signal processing to achieve the resolution required to isolate the signal of interest.
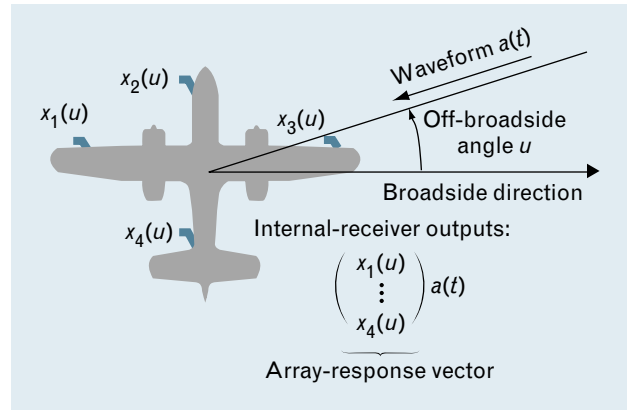
FIGURE 3. Geometry of a single emitter signal received at an aircraft with four antennas (in blue). The emitter transmits a time-dependent signal a(t), which arrives at an off-broadside angle u, where the broadside direction is defined as the two-dimensional geometric plane perpendicular to the flight path. The angle u and the waveform a(t) must be estimated for each emitter on the basis of the receiver outputs on the aircraft.

angle u, where the broadside direction is defined as the two-dimensional geometric plane perpendicular to the flight path. The off-broadside angle u and the waveform $a(t)$ must be estimated for each emitter on the basis of the receiver outputs on the aircraft.

Each of the four antenna elements on the aircraft has an antenna pattern for receiving the emitter signal; each antenna pattern depends on the aircraft structure and the presence of other antennas. The effective response of each antenna element is the superposition of its antenna pattern onto the simple phase difference that arises from the antenna's location with respect to a defined reference point on the aircraft. For example, the second antenna (near the nose of the aircraft in Figure 3) has an antenna response $x_2(u)$. The four outputs of the internal receivers of the aircraft are the products of the signal waveform $a(t)$ with the four antenna responses $x_1(u)$ through $x_4(u)$ in the direction u; the antenna responses form the array-response vector. When we have more emitters, the receivers sum their outputs linearly.

We express the receiver outputs mathematically as

$$\mathbf{z}(t)_{M\times 1} = \sum_{i=1}^{S}\left[\mathbf{x}_T(u_i)\,a_i(t)\right] + \mathbf{n}(t).$$

The vector of M baseband receiver outputs $\mathbf{z}(t)$ has two principal components: one from whatever emitters are on the channel, and the other from noise $\mathbf{n}(t)$, which can include receiver noise and background radiation. The component of the output from the emitters is a sum over S emitters, where each term in the sum is the product of an array-response vector $\mathbf{x}_T(u_i)$, and a waveform $a_i(t)$, where i denotes the ith waveform having direction u_i. The number of emitters S is unknown, and the background radiation may have some unknown parameters.

How well we can solve our parameter estimation problem depends on the degree of prior knowledge we have about the waveform and the array-response vectors. Waveform knowledge is defined as knowing (or correctly assuming) that the waveform of interest lies in some particular class. Examples of waveform classes are the generic signal, for when we know nothing about the waveform; almost constant envelope (ACE); single sideband (SSB); amplitude modulated (AM) or on-off keyed; time-varying power distribution (e.g., intermittent); and stochastic (i.e., random-appearing modulation).

For generic signals, we utilize the root-MUSIC (multiple signal classification) algorithm [1]. We also developed several direction-finding and signal-copy

algorithms that use prior knowledge of the waveform class [1]. In this article, we present experimental results for three algorithms. The cumulant eigenanalysis (CUE) algorithm can be used on stochastic waveforms that are non-Gaussian. The adaptive event processing (AEP) algorithm works for signals that are intermittent on a given frequency channel. In this context, an event refers to an emitter turning on or off. The waveform improved nulling (WIN) algorithm works on ACE, SSB, AM, or on-off keyed signals. All of these algorithms, known as copy-based, can perform signal copy without any array-response knowledge. However, array-response knowledge is needed for a copy-based algorithm to perform direction finding.

There are two categories of array-response vector knowledge. As with waveform knowledge, the first category corresponds to an unknown array-response vector. In this case, we can copy certain waveforms if we know something about the waveform, but we are

not able to direction-find the signal. The second category corresponds to an array-response vector derived from calibrating the array or from predicting the array-response vector as a function of angle. The error between the calibrated or predicted response and the actual response typically comes from two sources— the antenna patterns and the receiver channels. For an array that responds strongly to vertically and horizontally polarized signals, we may have to calibrate or predict its response for both kinds of polarization states. Our discussion initially focuses on the reception of vertically polarized emitters, which is what we expect to receive in the battlefield environment.

Errors in the antenna patterns depend on the direction of the emitter, and are represented by the matrix $\mathbf{B}_i$ for the ith emitter. Errors in the receiver channels are independent of the angle of arrival of the emitters, and are represented by the matrix $\mathbf{G}$. The matrix $\mathbf{B}_i$ of angle-dependent errors is different for each source, while the matrix $\mathbf{G}$ of angle-independent
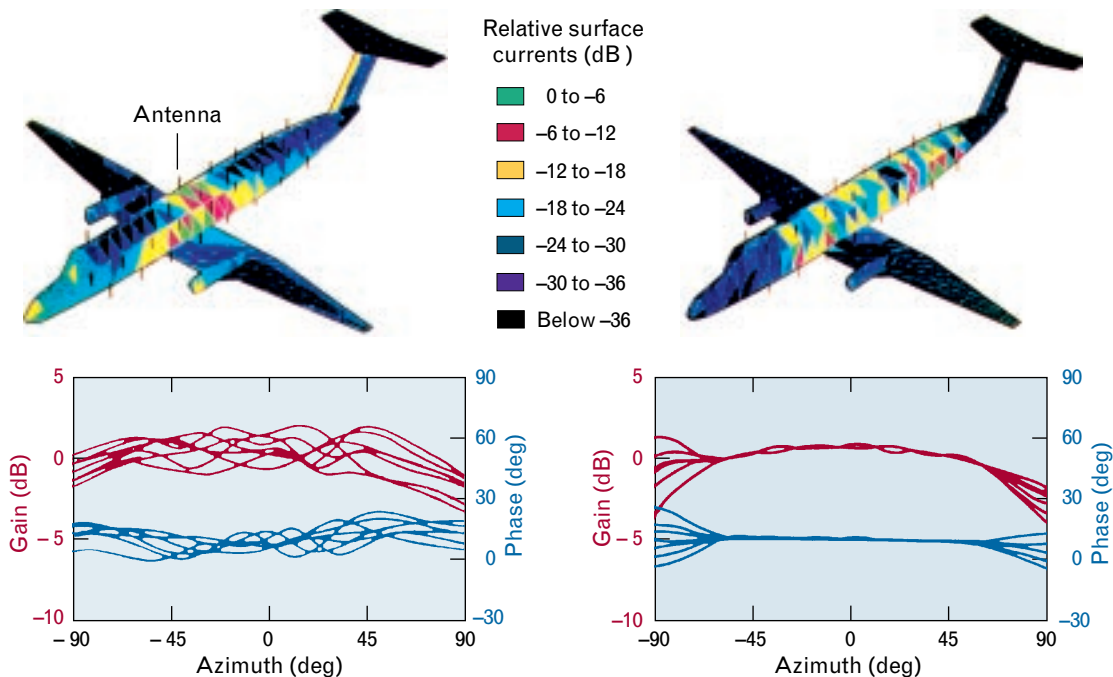
FIGURE 4. Surface currents that result when the fourth dipole pair is activated (top left). Substantial surface current is generated on the fuselage, and extraneous currents appear on the nose, tail, and engine nacelle toward the transmitting side. As each element is activated sequentially, the extraneous currents cause the antenna patterns to differ from one another (bottom left) and to exhibit slow undulations with azimuth angle. Through a technique called pattern response equalization for spatial similarity (PRESS), we create a smooth, matching antenna pattern (bottom right) for each antenna-element location by activating all of the elements with appropriate amplitude and phase adjustments. When we simulate the fourth antenna element with appropriate adjustments, the extraneous surface currents are reduced (top right), which produces the smooth pattern.

errors is the same for all sources. These matrices are diagonal and typically resemble identity matrices.

The true array-response vector of the ith source, $\mathbf{x}_T(u_i)$, differs from the calibrated or predicted array response $\mathbf{x}(u_i)$ through multiplication by the two error matrices:

$$\mathbf{x}_T(u_i) = \mathbf{B}_i \mathbf{G} \mathbf{x}(u_i).$$

Without errors, the $\mathbf{B}_i$ and $\mathbf{G}$ matrices would be identity matrices, and $\mathbf{x}_T(u_i)$ would be identical to $\mathbf{x}(u_i)$. Direction-finding algorithms in particular can be sensitive to small errors when the emitters are close together in beamwidths. Reducing these errors is a major technical challenge in our work.

Technical Challenges of Direction-Finding and Copying Generic Signals

In the generic-signal case, an ambiguous solution to the parameter-estimation problem results unless we have some prior knowledge of the array response. Furthermore, the direction-finding and copy algorithms that apply in this case work best when the antenna patterns match one another. We now discuss a signal processing technique that matches different antenna patterns. By observing the antenna patterns of transmitting antennas, we can determine the antenna patterns that occur when we receive signals. Figure 4 shows the effect of activating one element of an antenna array aboard an aircraft. The antenna array comprises eight pairs of dipoles that span the left and right sides of the fuselage; each dipole element projects out of the top and bottom of the aircraft. The dipoles can be phased such that their emitted energy goes toward either the port or the starboard side of the aircraft. In the upper-left part of Figure 4, the dipoles are phased to direct the energy to the port side; we are transmitting with the fourth antenna element back from the nose of the aircraft.

By using the Finite Element Radiation Model (FERM) software developed at Lincoln Laboratory [2], we can study the currents that are generated on the surfaces of the aircraft when any antenna element is activated. When the fourth antenna element is activated, substantial current is generated on the fuselage near the activated element, as expected. However, we also see significant extraneous current generated on the nose of the aircraft, on the tail, and on the engine nacelle toward the transmitting side. As each antenna element is activated in turn, these extraneous currents cause the antenna patterns (shown for vertical polarization) to vary with azimuth angle, and to differ from one another.

The bottom left of Figure 4 shows the varying gain and phase patterns for each of the eight antenna elements. The peak-to-peak variations are approximately 3 to 4 dB in gain and about 20° in phase. The undulations in these antenna patterns are relatively slow as a function of azimuth angle because the aircraft is only a few wavelengths long. We can create a smooth, matching antenna pattern for each antenna-element location by activating all elements with appropriate amplitude and phase adjustments. This smoothing process is called the pattern response equalization for spatial similarity (PRESS) technique because it effectively presses the antenna patterns.

The PRESS technique can be implemented either by expressing the smooth antenna responses as linear combinations of the true, undulating responses or by expressing the true responses as linear combinations of the smooth, ideal responses, which constitutes a truncated, Fourier-type series representation of the true responses. For example, to simulate the fourth element with a smooth pattern in this experiment, we used the set of adjusted amplitudes and phases for all elements. Because we were using all of the elements, the top right of Figure 4 shows current all along the fuselage of the aircraft; however, because little current passes through the nose, tail, and engine nacelle, the antenna-pattern undulations disappear. The bottom right of Figure 4 shows antenna patterns that match one another well over the specified angular region from –60 to +60° in azimuth.

Test Results of Generic-Signal Algorithms and Algorithms That Use Waveform Knowledge

Lincoln Laboratory conducted an airborne technology demonstration simulating battlefield parameters to test the generic and three copy-based algorithms. Figure 5 shows major components of the demonstration system that we developed. Three test emitters were experimentally controlled to turn on and off in combinations, which allowed us to vary the experi-

ments and assess copy performance. These controlled emitters were supplemented by up to four additional emitters that were continuously on. All emitters were modulated with frequency modulation (FM) by voice or by noise, and were approximately 10 kHz in bandwidth. The emitters of interest had array signal-to-noise ratios [1] of nominally 40 dB. Their off-broadside angles ranged from –60° to 60°, and their depression angles ranged from 2° to 16° (not requiring calibration as a function of depression angle).

We equipped a Beechcraft 1900 aircraft with an inertial navigation system to sense the orientation of the aircraft. The aircraft also communicated with distance-measuring transponders on the ground to establish its location accurately. With this information and the exact coordinates of the test emitters, we knew the true directions of the emitters when their signals arrived at the aircraft. We could then compare the true directions with direction estimates from the direction-finding algorithms to assess the accuracy of the algorithms. We mounted a linear array of eleven antenna elements under radomes along the top and bottom of the fuselage and used various subsets of this array. The three additional dipoles shown in Figure 5 allowed us to generate linear and nonlinear arrays by using combinations of antenna elements.

Figure 6 shows the aircraft (left) with antenna elements mounted top and bottom along the fuselage under radomes. Each antenna element consists of a top and bottom pair that acts as a dipole. The slot-patch monopole antenna elements can be switched to have primary gain toward the starboard or port side. The inset at right shows the antenna elements with the radomes removed. The elements were designed to receive primarily vertical polarization.

Figure 7 shows the direction-finding and signal-copy results from a flight test. In this experiment, we used three ground emitters and four antenna elements to duplicate a battlefield situation. This 1.1-wavelength array was nonlinear, consisting of two an-
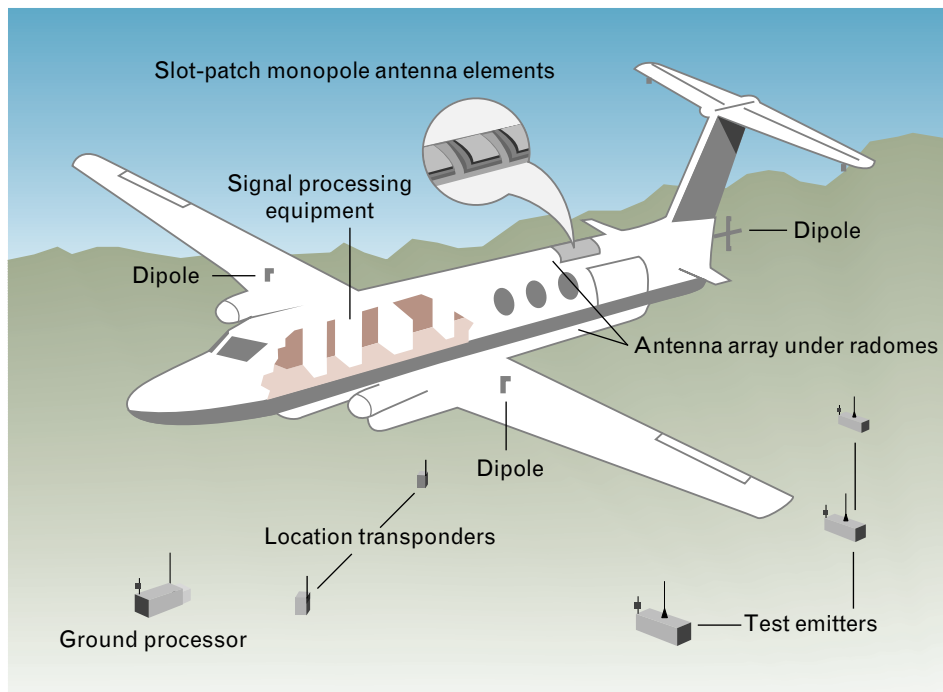
FIGURE 5. Components of the demonstration system. Three test emitters on the ground were activated and deactivated in various combinations to vary the experiments and assess copy performance. These controlled emitters were supplemented by up to four additional test emitters that were continuously on. The aircraft was outfitted with a linear array of eleven antenna elements, each consisting of a top- and bottom-mounted pair. The addition of three dipole elements allowed us to also test nonlinear array configurations.

FIGURE 6. Beechcraft 1900 aircraft (left) configured for the technology demonstration. An array of eleven antenna elements is mounted under radomes along the top and bottom of the fuselage in pairs that act as dipoles. The inset (right) shows the antenna elements without radomes.

tennas on the fuselage and the two dipoles on the wings. We first consider performance with the root-MUSIC algorithm for generic signals. The test scenario is challenging for generic-signal algorithms because the number of generic signals to direction find can at most equal one less than the number of antenna elements, although some forms of prior knowledge of the signals allow this bound to be relaxed.

A generic algorithm determines direction-finding estimates first, then copies the signals. The upper half of Figure 7 shows the off-broadside angles of arrival in beamwidths (BW) or degrees of the three emitters—

E_1, E_2, and E_3—in blue dashed lines during one flight leg as a function of time along the abscissa. Near the end of the flight test, the two closest emitters were less than one-tenth of one beamwidth apart, which represents a challenging situation. In addition, the middle emitter (E_2) has a power level that is approximately 20 dB down from the other emitters. Also shown at top are the direction-finding results (red Xs) for the root-MUSIC algorithm. A direction-finding and copy trial was conducted every 10 sec during the flight. The data collection interval for each experiment was 16 msec, yielding approximately 160
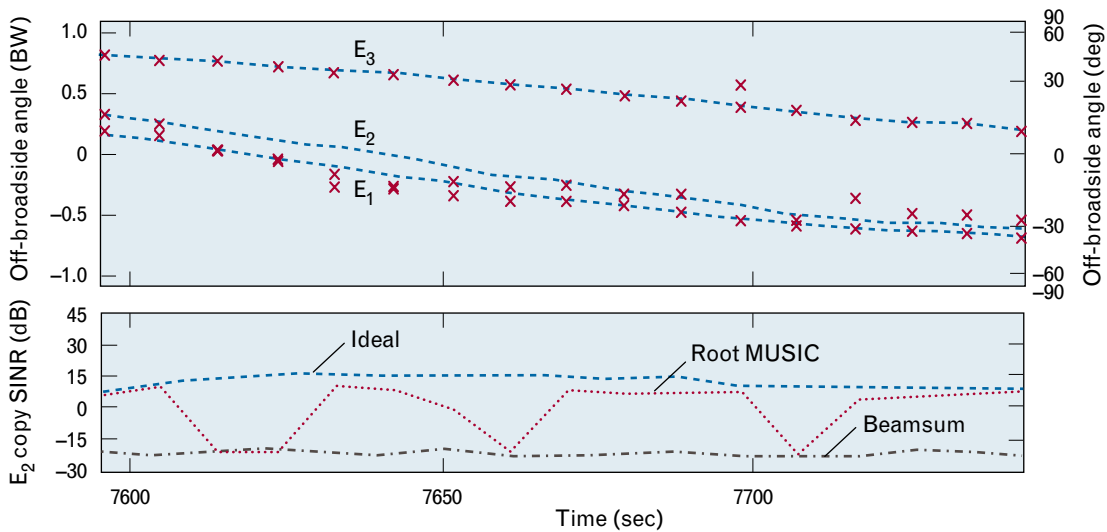
FIGURE 7. Direction-finding estimates from the root-MUSIC (multiple signal classification) algorithm (top) and copy performance (bottom) from an experimental battlefield scenario of three emitters and four antenna elements. The off-broadside angle is expressed in units of beamwidths (BW) on the left and degrees on the right. The root-MUSIC algorithm makes no assumptions about the classes of the waveforms of the emitters. Direction-finding and copy performance are seen to be reasonably reliable but not perfect. The traditional beamsum performance is shown here as a reference.

independent, simultaneous observations of the receiver outputs. The root-MUSIC algorithm determines reliable but not perfect directions; the direction-finding estimates for E_1 and E_3 are generally good, while direction estimates for the middle emitter E_2 are less accurate.

The lower half of Figure 7 shows copy performance for E_2, the weakest emitter, in terms of the output signal-to-interference-plus-noise ratio (SINR) [1] over time from the array. The ideal curve represents the best possible copy we can achieve with amplitude and phase adjustments on the element outputs. These adjustments form an array pattern that places antenna pattern nulls on the interferers while maintaining gain on the signal of interest. A level of 5 dB is sufficient for intelligible voice output from an FM emitter, and the ideal curve is above the intelligible level of 5 dB. The beamsum curve represents the SINR that we would get if we simply pointed a beam at the signal of interest. Because the signal of interest is much weaker than the other signals, this beamsum

performance is poor. The root-MUSIC algorithm SINR is over 5 dB most of the time, but has some dropouts and does not stay near the ideal copy level.

Figure 8 compares the performance of the root-MUSIC algorithm for generic signals (far left) with the performance obtained by using the CUE, WIN, and AEP algorithms for the same flight leg considered previously. These three algorithms utilize knowledge of the waveform class, perform signal copy prior to direction finding, and use no knowledge of the array response when copying the signal. All three algorithms achieve excellent signal copy, close to ideal. Over a broader set of scenarios not shown, the WIN and AEP algorithms perform more closely to ideal than does the CUE algorithm. For direction finding, the WIN algorithm gives the best estimates, and its performance was quite good even in this extremely difficult scenario with the two closest emitters less than a tenth of a beamwidth apart. Both the CUE algorithm and the AEP algorithm had a mixed performance for direction finding.
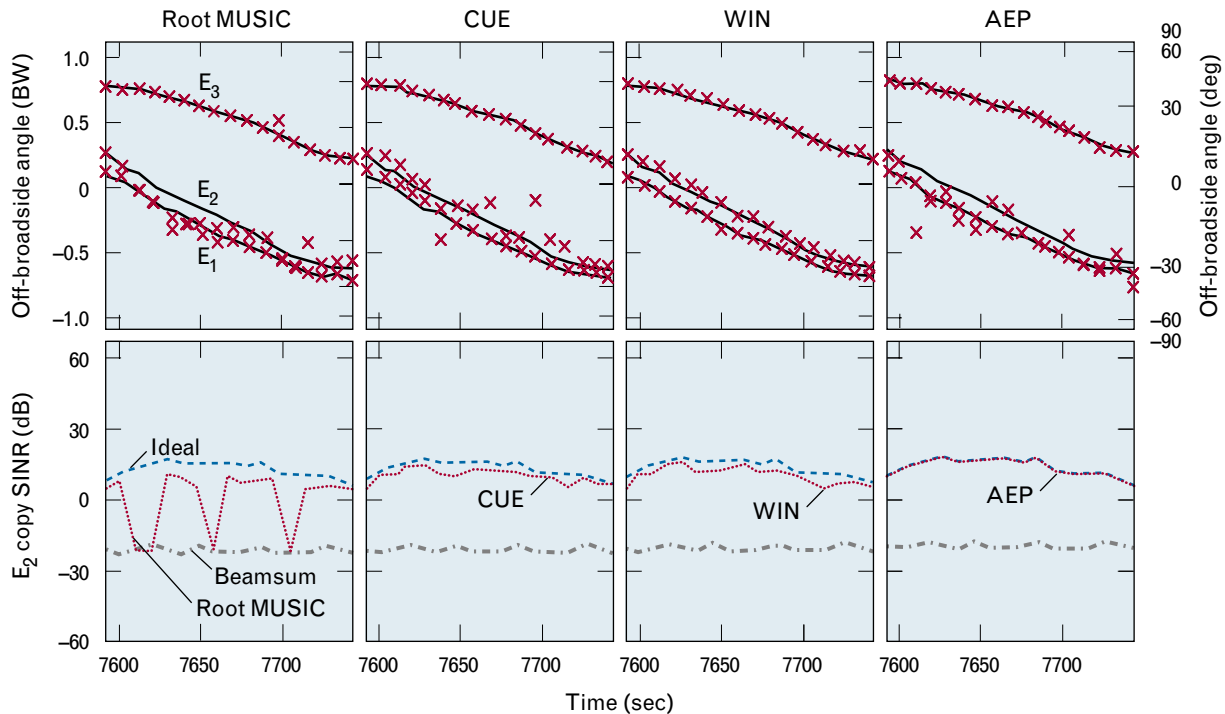
FIGURE 8. Comparison of direction-finding and copy performance for the root-MUSIC, cumulant eigenanalysis (CUE), waveform improved nulling (WIN), and adaptive event processing (AEP) algorithms. The traditional beamsum performance is shown here as a reference. The three copy-based algorithms perform signal copy prior to direction finding, and yield copy performance close to ideal in this scenario. All the algorithms perform better than root MUSIC in this regard. For direction finding, WIN performs the best.

Benefits of Enhanced Array Calibration

We can improve the performance of direction finding and some copy algorithms by using enhanced calibration of the array response. Figure 9 shows the antenna patterns of six of the elements on the aircraft (i.e., every other antenna element of the linear array). For these calibration measurements, data from three vertically oriented sources were used. The figure shows amplitude variations as a function of off-broadside angle at top, and phase at bottom. We see peak-to-peak variations of approximately 3 to 4 dB and approximately 20°, similar to the FERM results of Figure 4. Here, the dominant undulations are reasonably slow, as we expect, given the size of the aircraft (three wavelengths); however, we also observe that there are some rapid variations. We assumed on the basis of various tests we made on the antenna patterns that the rapid variations were caused by fluctuations in the polarization states of the calibration sources—local multipaths near the sources could cause such variations of the received polarization state (even though our sources were vertically oriented). To solve this problem, we designed a calibration technique that allowed the polarization states to vary, and we solved for these states during the calibration process, which was performed by using emitters with different polarizations. This technique is called double PRESS.

Figure 10 shows the residual calibration errors for various calibration techniques. Each point shown comes from a measurement at a different off-broadside angle, as shown on the abscissa. If we use just the element locations and no calibration at all, the errors (red Xs) are typically 16 dB below the patterns (phase errors per element of approximately 6°). With the PRESS technique, however, we typically get residuals 30 dB down (phase errors per element of approximately 1.3°). These residuals correspond to the rapid variations shown in Figure 9. For the two versions of PRESS calibration, the angle-independent errors were kept extremely low through periodic (every 10 sec) receiver-channel calibration; because of date-to-date drifts of the calibration channels, and required maintenance actions, single-emitter data from a few emitters were used to realign the calibration channels for each flight experiment. Thus the residuals shown
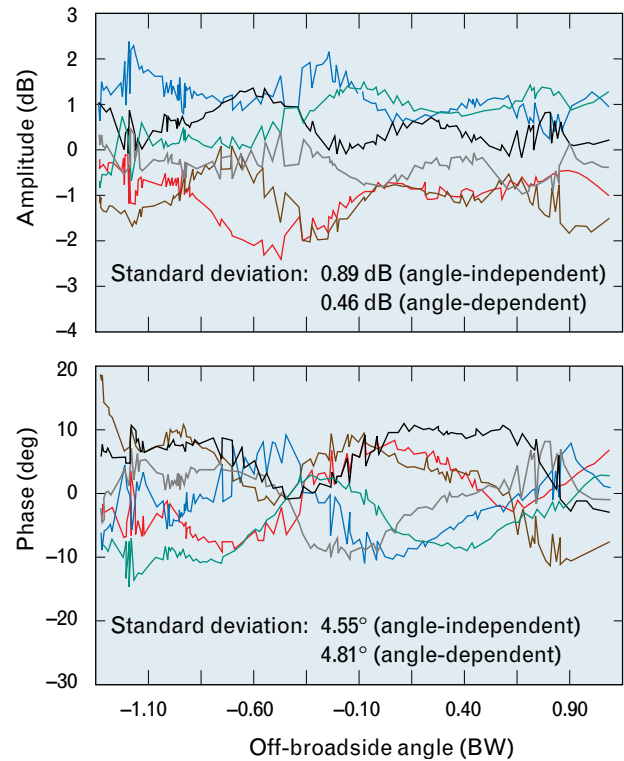
FIGURE 9. Measured antenna patterns from six aircraft antenna elements. Three vertically oriented sources were used in the experiment. The slow undulations in the patterns resemble those seen in Figure 4, and the rapid variations are caused by fluctuations in the received polarization states. The rapid variations were accounted for by redesigning the calibration technique.

here for PRESS and double PRESS are the angle-dependent errors. With the double-PRESS technique, which accounts for possible polarization-state variations of the calibration sources, we are typically able to bring the errors down 41 dB (phase errors per element of approximately 0.4°). We used two-month-old antenna calibration modeling to show that the demonstration system did not require frequent antenna pattern calibration, which indicates the high quality of the demonstration system hardware.

Figure 11 shows the improvement in accuracy obtained from using the double-PRESS calibration in conjunction with appropriate direction-finding and signal-copy algorithm versions in a three-emitter flight test with six elements from the linear array on the aircraft. (In these experiments, a 20-msec data collection interval was utilized, and results are shown every 20 sec.) The emitters were all nominally verti-
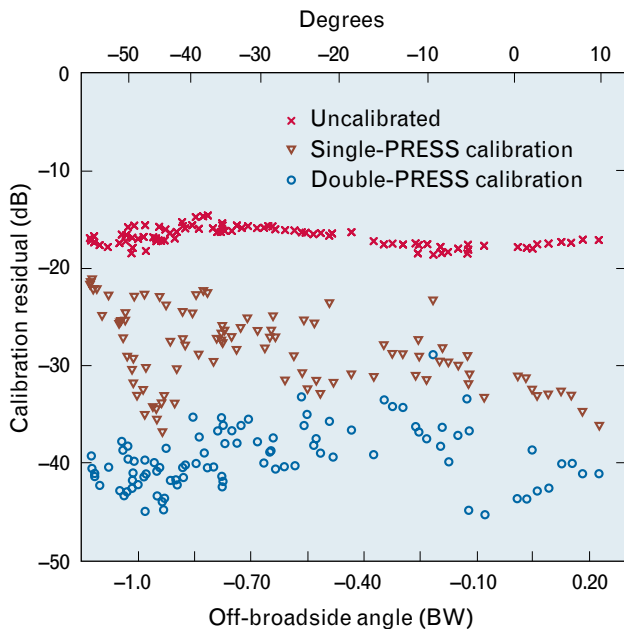
FIGURE 10. Residual errors for different antenna-calibration techniques. The red Xs correspond to calibration modeling that knows the antenna-element locations but assumes the elements have isotropic antenna patterns. These errors are too large to support good direction finding for the scenarios considered in this article. Using single PRESS reduces the errors significantly, yielding the type of direction-finding and copy performance seen in Figure 8. With double PRESS, the residual errors are further reduced, resulting in the excellent direction finding and copy in Figure 11.

cally polarized. For this experiment, the total aperture length was 1.1 wavelengths and the emitters were of equal power levels. We present two before-and-after cases. On the left half of Figure 11, we compare the PRESS calibration technique with double PRESS for generic signal algorithms. The polarization-diverse MUSIC algorithm is a modified version of that in Reference 3; it uses points of inflection of the MUSIC spectrum for enhanced resolution. On the right half, we compare PRESS with double PRESS for the AEP algorithm [1]. For the generic-signal case on the left, the direction-finding estimates are greatly improved by the calibration enhancement. Performance is excellent even though the emitters are at times less than 0.1 beamwidths apart. To show the improvement in all the direction estimates, we provided the algorithms with the exact number of emitters for this test flight. The signal-copy performance is also greatly improved, as we see from the red curves. For AEP,

which works with intermittent signals and performs copy without array calibration, copy is always good. For direction finding, however, the enhanced calibration helps dramatically. The antenna calibration modeling in these experiments was two months old.

Implications for Battlefield Intercept

Figure 12 shows what we can accomplish with combinations of waveform and array-response knowledge for the multiple-emitter scenarios discussed in the article. For example, with prior knowledge of the waveform but no knowledge of the array response, we can achieve an excellent copy of the signal. When we have good array calibration, even with generic signals, we can reasonably direction-find and copy signals. Finally, we see that direction finding is greatly enhanced when the array calibration is enhanced.

On the basis of our successful experiments with emitters separated by less than a tenth of a beamwidth, and on a separate (unpublished) analysis of stressful battlefield signal interception, we conclude that successful detection, direction finding, and copy can be achieved, given one to three wavelengths of aperture and four to eight antenna elements to handle the cochannel interference. We are able to obtain acceptable performance with all signal types in the low VHF band. Our choice of algorithms and system design depends on the signal types of interest. Similarly, system configuration, size, and weight are mission driven, but we can obtain a small, lightweight implementation for narrowly focused missions. These techniques can be used to upgrade current signal intercept systems.

Acknowledgments
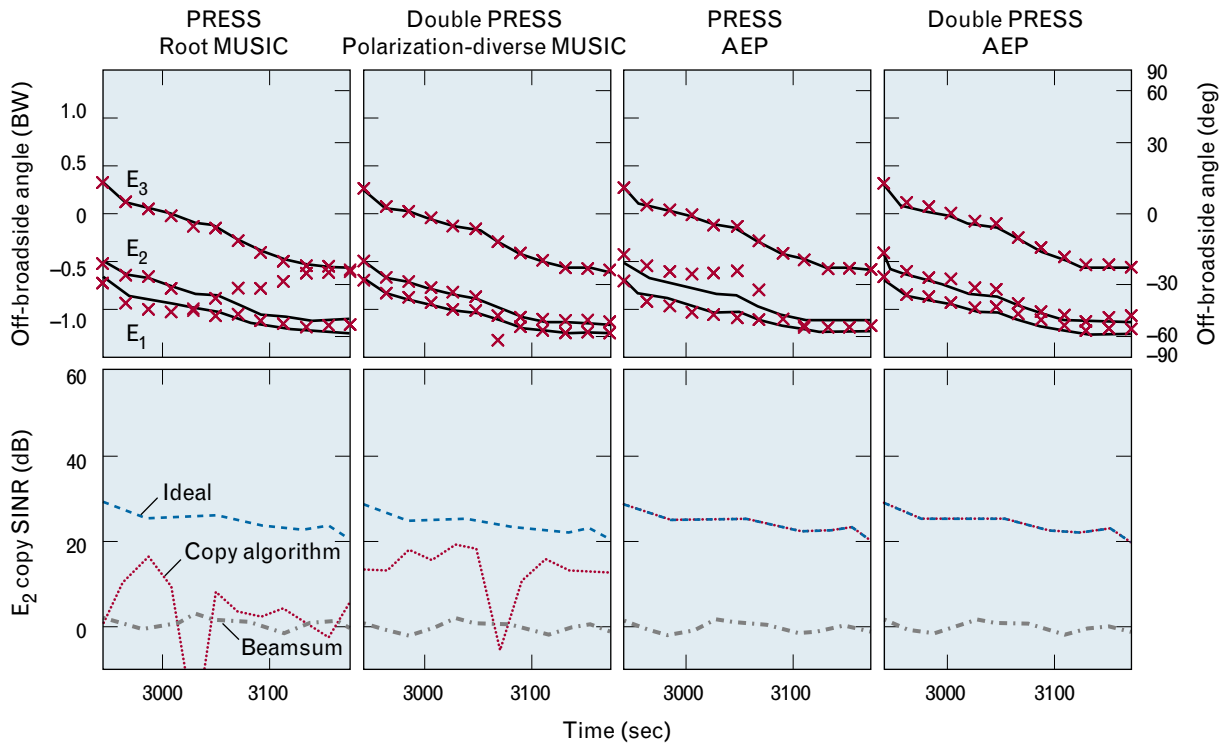
FIGURE 11. Comparison of direction-finding and copy performance from algorithms that use PRESS antenna-calibration modeling with those which use double PRESS. The left two panels are a before-and-after case for generic signals. Both direction-finding and copy performance are significantly enhanced. The right two panels show direction-finding and copy performance for the AEP algorithm for intermittent signals. Even though the AEP algorithm does not use array calibration for copy, the direction-finding estimates are greatly enhanced.

FIGURE 12. Direction-finding (DF) and copy capabilities for combinations of waveform and array-response knowledge.

REFERENCES

1. K.W. Forsythe, "Utilizing Waveform Features for Adaptive Beamforming and Direction Finding with Narrowband Signals," *Linc. Lab J.,* in this issue.
2. D.A. Shnidman and S. Lee, "The Finite Element Radiation Model (FERM) Program," *Conf. Proc. 3rd Annual Review of Applied Computational Electromagnetics, Monterey, Calif., 24–26 Mar. 1987,* session IV.
3. E.R. Ferrara, Jr., and T.M. Parks, "Direction Finding with an Array of Antennas Having Diverse Polarizations," *IEEE Trans. Antennas Propag.* **31** (2), 1983, pp. 231–236.

LARRY L. HOROWITZ
is a senior staff member in the
Advanced Techniques group.
He researches performance
bounding and signal process-
ing algorithm development for
adaptive sensor systems and
performance bounding for
automatic target recognition
with advanced synthetic-
aperture radar data. Before
joining Lincoln Laboratory in
1975, Larry worked for The
Johns Hopkins Applied Phys-
ics Laboratory in performance
analysis of single-bit receivers
of global positioning system
(GPS) satellite signals.

Larry received S.B., S.M.,
and Ph.D. degrees in electrical
engineering from MIT. He
held a National Science Foun-
dation Graduate Fellowship
from 1972 to 1974.